

International Journal of Modern Physics D
 © World Scientific Publishing Company

**PROBING COLD DARK MATTER CUSPS
 BY
 GRAVITATIONAL LENSING**

V. K. ONEMLI

*Department of Physics and Institute of Plasma Physics, University of Crete,
 Heraklion, GR-710 03, Greece
 onemli@physics.uoc.gr*

Received Day Month Year
 Revised Day Month Year
 Communicated by Managing Editor

I elaborate on my prediction that an indirect detection of cold dark matter (CDM) may be possible by observing the gravitational lensing effects of the CDM cusp caustics at cosmological distances. Cusps in the distribution of CDM are plentiful once density perturbations enter the nonlinear regime of structure formation. Caustic ring model of galactic halo formation provides a well defined density profile and a geometry near the cusps of the caustic rings. I calculate the gravitational lensing effects of the cusps in this model. As a pointlike background source passes behind a cusp of a cosmological foreground halo, the magnification in its image may be detected by present instruments. Depending on the strength of detected effect and the time scale of brightness change, it may even be possible to discriminate between the CDM candidates: axions and weakly interacting massive particles.

Keywords: Dark matter; cusp caustics; gravitational lensing.

1. Introduction

Caustics of light¹ are generically the enveloping surfaces of a family of light rays where the intensity is high. Such concentration of light can burn, hence these envelopes are called “caustics.” The caustic formation in the propagation of light is a common phenomenon in nature. Rainbows, scintillation of stars, shimmering of the sea and dancing patterns of bright lines that appear on the bottom of a swimming pool are among the most familiar examples. When the wavefront of sun light enters into water, it gets retarded proportional to the local thickness of the wavy surface. If the thickness is small, the amplitude of the wavefront is not affected much, hence, the density of light rays remains almost uniform just under the water surface. In a deeper level from the surface, however, the rays necessarily intersect each other, because the tiny deviations in the paths of the rays due to the refraction are amplified. They form cusp-shaped regions bounded by an enveloping surface of rays. Three light rays hit every point inside this region, whereas one light ray hits

2 *V. K. Onemli*

every point outside. The enveloping surfaces, where the number of light rays jumps by two, are the fold caustics of light. Cusps occur wherever the folds merge. The density diverges when a caustic is approached from the side with extra rays; see Section 2. Thus, a mild modulation in the wavefront spontaneously generates a strong enhancement in intensity some distance away, at caustic locations. Caustics move about but remain robust under stirrings of the water surface.

Caustics are common in the propagation of light, because (i) photons are classically *collisionless*, and (ii) flow of light from a distant (pointlike) source has zero *velocity dispersion*. Caustics of ordinary luminous matter is unusual, because ordinary matter is normally collisionful. However, the fall of stars in and out of a galactic gravitational potential well is collisionless. Many elliptic galaxies are surrounded by ripples² in the distribution of light that are interpreted as caustics of luminous matter.³ These ripples provide an *existence proof* of discrete flows and caustics in the infall of ordinary matter which constitutes only 4% of the content in the Universe. It is believed that 22% of the composition consists of nonluminous, *collisionless* particles with very small *primordial velocity dispersion*.⁴ Such particles are called cold dark matter (CDM). The leading CDM candidates are axions and weakly interacting massive particles (WIMPs). Galaxies are surrounded by CDM that keeps falling into the gravitational potential wells of galaxies from all directions and forms halos around their baryonic disks. Because the number densities of axions and WIMPs are huge, their infall onto isolated galaxies is regarded as a continuous flow. The number of flows, however, is discrete^{5,6} at any point in the halo and changes as a function of space and time. The enveloping surfaces where the number of flows jumps by two are the CDM caustics. Sharp discontinuities in the CDM density distribution occur at the locations of the caustics. Existence of caustics in such a CDM infall^{7–11} can be taken for granted, once the existence of ripples³ in the infall of ordinary matter is given. In a typical galaxy, any effect one can imagine that may erase CDM caustics, would have already erased these ripples. Indeed, there are several evidences for CDM caustics found in the halos of galaxies including the Milky Way.^{12–14}

There are at least two sets of caustics in the halos of isolated galaxies: outer caustics and caustic rings.^{8–10} Outer caustics are simple fold (A_2) catastrophes located on topological spheres enveloping the galaxy. Caustic rings, on the other hand, are closed tubes whose transverse cross-section is a closed line with three (dual) cusps, called a “tricuspid.” One of the cusps, the outer cusp, lies in the galactic plane, the other two are nonplanar; see Fig. 1. The triaxial tricuspid is called elliptic umbilic (D_{-4}) catastrophe.

To see the caustic formation^{8–10} in the infall of CDM, consider the time evolution of CDM particles that are about to fall into the potential well of an isolated galaxy at time t_1 for the first time in their history. They form a topological sphere with radius $R_1(t_1)$ enclosing the galaxy called the “turnaround” sphere at time t_1 . After falling all the way through the disk of the galaxy, the particles of this turnaround sphere form a new sphere which reaches its maximum radius $R_2(t_2)$ at time t_2 .

$R_2(t_2) < R_1(t_1)$ because of the deepening of the potential well in the meantime. Note also that, due to the growth of the galaxy, the first turnaround radius $R_1(t_2)$ at

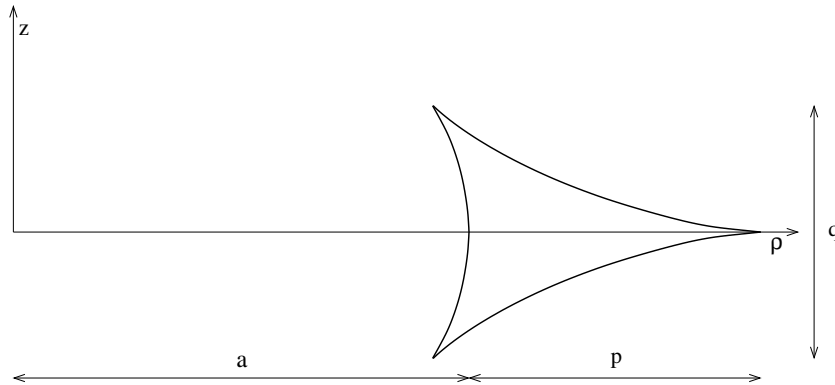


Fig. 1. Cross-section of a caustic ring in the case of axial and reflection symmetry. ρ and z are galactocentric cylindrical coordinates. p and q are the transverse dimensions in the $\hat{\rho}$ and \hat{z} directions, respectively. a is the ring radius. p and q are taken of order a , for clarity. $p, q \ll a$ for actual caustic rings.

time t_2 is larger than $R_1(t_1)$. The sphere continues to oscillate in this way. Therefore, there are discrete number of flows in and out of the galaxy at any location in the halo. The local number of flows increases, as one approaches the galactic center from an arbitrary direction at a given time. First, in the outermost regions, there is one flow (particles falling in for the first time), then, at a certain location, the number jumps to three (particles falling in for the first time, particles falling out for the first time, particles falling in for the second time), and then to five, to seven, and so on, at other certain locations closer to the center. The boundary—which is a topological sphere—between the region with one (three, five, . . .) flow and the region with three (five, seven, . . .) flows is the first (second, third, . . .) outer caustic. Outer caustics are simple fold catastrophes. In the limit of zero velocity dispersion, the density diverges when the outer caustics are approached from the side with two extra flows; see Section 3. To see the formation of caustic rings with tricusp cross-section, on the other hand, a closer inspection to the time evolution of the infall sphere is needed.^a Notice that, each time the turnaround sphere falls through the galaxy, it turns itself inside out.^{8–10} The particles near the equator of the infall sphere carry too much angular momentum to reach the central part of the galaxy, and therefore, just before the sphere turns itself inside out, there exists a circle of points which are inside the sphere last. This circle is the locus of outer cusps that lie in the plane of the galaxy (see Fig. 1). Hence, caustic rings are located near where the particles with the most angular momentum in a given inflow reach their

^aSee Ref. 10 for details.

4 *V. K. Onemli*

distance of closest approach to the galactic center before going back out.¹⁰ Because the CDM infall is continuous, the caustic ring in space-time associated with the infall sphere is a persistent feature in space. There is a caustic ring due to CDM particles falling through the galaxy for the first time, a caustic ring of smaller radius due to particles falling through for the second time, and so on. Like outer caustics, caustic rings are boundary surfaces where the number of flows jumps by two. Inside the caustic rings there are four flows, whereas there are two flows outside.

Caustic structure in the dark matter infall may be revealed by observing their gravitational lensing effects.^{15–19} The effects are largest near the cusps¹⁹ which are common features in the halo CDM distribution.^b In this paper, I review the lensing effects near the cusps of caustic rings.¹⁹ The outline is as follows. In Section 2, caustics in the propagation of light are introduced. They provide a useful analog for understanding the properties of caustics in the infall of cold dark matter. The outer caustics and caustic rings of CDM are reviewed in Section 3. Their gravitational lensing effects are discussed in Section 4. Conclusions are summarized in Section 5.

2. Caustics of Light

When natural processes focus light, the caustics that are generated have a systematic pattern.¹ The mathematical tool to investigate this systematics is the catastrophe theory which analyzes the different ways that the critical points of gradient mappings can merge to make higher singularities. In optics, the mappings are from an incident wave front to the space in which the wave is observed; i.e. three-dimensional (3D) space around the caustic or 2D space of a screen. The quantity that is extremized is the Fermat’s potential and the critical points correspond to the light rays. The annihilation of two critical points at a location by coalescence with each other means loss of two rays contributing to a focus at that location.

Caustics spontaneously arise when a forefront object distorts the propagation of light from a distant (pointlike) source. Although the light rays are parallel initially, they necessarily cross each other after the distortion and produce caustics systemized as folds and cusps. If an observer places his/her eye inside the region bounded by two folds that merge at a cusp, light rays enter eye from three distinct directions, each corresponding to an image of the source. Every point outside the region, on the other hand, is hit by one ray only. A 2D cross-section of such a region is depicted in Fig. 2. Thus, as the point of observation crosses a fold caustic surface, the number of images jumps by two. If the eye moves from the inside across one of the folds, two of the images approach each other increasing in brightness, coalesce at the fold and then disappear outside. Meanwhile, the third image remains pretty much the same. If the eye moves towards the other fold, the third image coalesces

^bFor example, gravity of massive objects like stars, focus the CDM flow producing a cone-shaped caustic surface —whose apex is a cusp— near the trajectories of maximum scattering angle.²⁰ This effect can be generalized considering an isolated galaxy or even an isolated (super)cluster of galaxies as a massive object, as a whole.

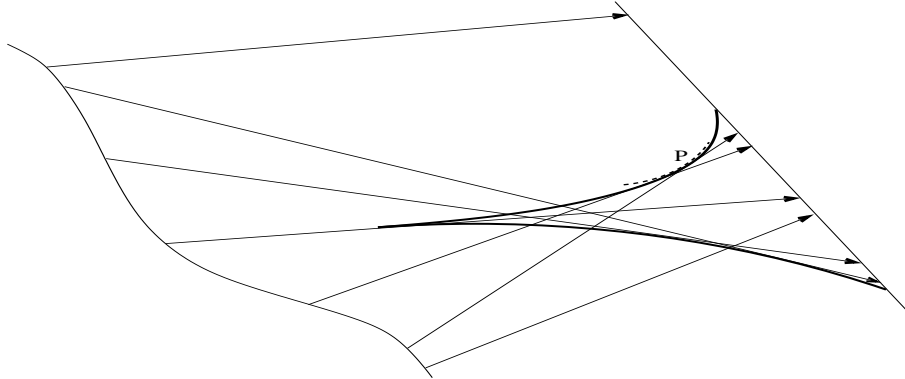


Fig. 2. Distribution of light rays in the vicinity of a two dimensional cut of a region bounded by two folds merging at a cusp. The local curvature radius R of the fold at point P along the tangential direction is that of the circle depicted by dashed lines.

with one of the other two images at the fold and then disappear. The closer the eye is to the cusp, the closer the two images are. The three images merge at the cusp. Because rays are more concentrated near the cusps, the intensity is largest there; see Fig. 2. When a fold is approached from the side with two extra rays at every point, the density rises as $\sigma^{-1/2}$ in the vicinity of the fold, where σ is the distance to the fold in the direction of approach. This can be seen as follows. The rays tangent to a small segment of a smooth caustic fold at a point P are uniformly distributed¹ along it; see Fig. 2. The corresponding length of the segment $\simeq 2\sqrt{2R\sigma}$ where R is the local curvature radius of the fold at P along the tangential direction. Therefore, in the caustic neighborhood, the number of rays N passing between the observer and the fold is proportional to $2\sqrt{2R\sigma}$. Hence, the number density $dN/d\sigma \sim \sigma^{-1/2}$. Because caustics of light form spontaneously in rather general circumstances and retain their identity under perturbations, they are generic and structurally stable.

3. Caustics of Cold Dark Matter

CDM infall onto isolated galaxies *intrinsically* has the necessary conditions for the caustic formation noted in Section 1: (i) the particles interact only weakly, and (ii) the primordial velocity dispersions δv of the CDM candidates are of a very small order. For the axion infall, the primordial velocity dispersion at time t , is of order^{8,21} $\delta v_a(t) \sim 10^{-12} \text{ km/s} (10^{-5} \text{ eV}/m_a)^{5/6} (t_0/t)^{2/3}$, where t_0 and m_a are respectively the present age of the Universe and the axion mass. For the WIMP infall, $\delta v_\chi(t) \sim 10^{-6} \text{ km/s} (\text{GeV}/m_\chi)^{1/2} (\text{MeV}/T_D)^{1/2} (t_0/t)^{2/3}$, where T_D and m_χ are respectively the decoupling temperature and the mass of the WIMPs.^{8,10} (Detailed derivations of δv_a , and δv_χ —including the possible effect of reheating by the e^-e^+ annihilations—can also be found in Ref. 17). Thus, stable and generic caustic formation in the CDM infall is inevitable, once density perturbations enter the nonlinear regime. In this section, I review the properties of the minimal caustic structure^{8–10} that must occur

6 *V. K. Onemli*

in galactic halos: outer caustics and caustic rings.

3.1. *Outer caustics*

Outer caustics are topological spheres enveloping the galaxies. In catastrophe theory, they are known as simple fold (A_2) catastrophes. To derive the properties of the

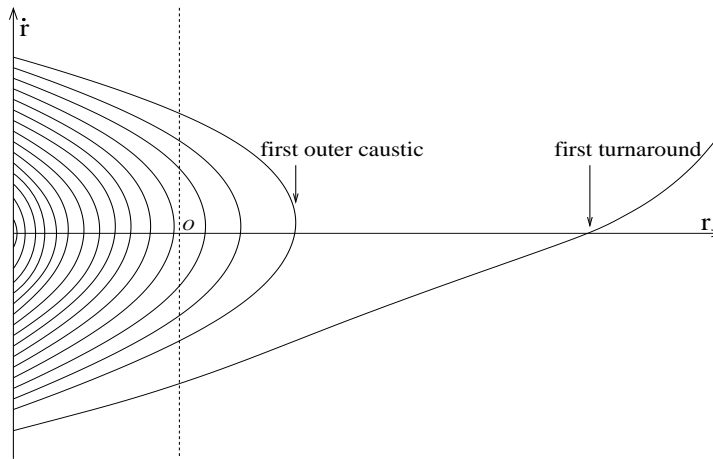


Fig. 3. Snapshot of the phase space of CDM particles in a galactic halo. r is galactocentric distance and \dot{r} is radial velocity. The solid line indicates the location of the particles. The dotted line corresponds to observer position. Each intersection of the solid and dotted lines corresponds to a CDM flow at the observer’s location O . Caustics occur wherever the phase space line folds back.

outer caustics, it is instructive to discuss their formation in the phase space point of view.^{8–10} The small velocity dispersion δv means that CDM particles lie on a very thin 3D sheet in 6D phase space. The thickness of the sheet is the δv of the particles. The flows can be described in terms of the evolution of this sheet.^{5,8} Figure 3 depicts two dimensional cut (r, \dot{r}) of the phase space, r being the radial coordinate and \dot{r} being the radial velocity.⁸ Before density perturbations enter the nonlinear regime of structure formation, there is only one flow (i.e. a single value for velocity) at a typical location in physical space. When a large overdensity enters the nonlinear regime, the particles in the vicinity of the overdensity fall back onto it. This implies that the phase space sheet winds up in phase space wherever overdensity grows. The outcome of this process is an odd number of discrete flows at any point in a galactic halo; see Fig. 3. Between the first turnaround^c radius and the location where the phase space sheet folds back for the first time —near^d the second turnaround

^c“Turnaround” refers to the moments in a particle’s history when it has zero radial velocity with respect to the galactic center.

^dThe n -th fold is located near the $n+1$ -th turnaround radius; see Fig. 3. If the flow were stationary the n -th fold would be located exactly at the $n+1$ -th turnaround radius.

radius— there is one flow (associated with particles falling in through the galaxy for the first time). Between the first and second folds there are three flows (associated with particles falling in through the galaxy for the first and second times, and with particles falling out of the galaxy for the first time). Between the second and third folds there are five flows and so on. (Wherever the phase space sheet folds back, the number of flows in physical space jumps by two naturally). The surface in physical space which envelopes the region with the two extra flows, associated with the corresponding fold of the phase space sheet, is a CDM caustic. At the fold, the phase space sheet is tangent to velocity space, particles pile up there and the physical space density diverges as the inverse square root of the distance σ to the caustic, when it is approached from the side with the two extra flows. This can be shown as follows.¹⁷ The 2D phase space mass density near a fold may be represented as $d^2M/d\sigma d\dot{\sigma} = M\Theta(\sigma)\delta(\sigma - (C\dot{\sigma})^2)$, where C and M are positive numbers; see Fig. 3. The direction of σ coordinate is chosen pointing inward. The density is the integral of the phase space density over velocity space

$$d(\sigma) = M \int d\dot{\sigma} \frac{\Theta(\sigma)}{2C} [\delta(\dot{\sigma} - \sigma^{1/2}/C) + \delta(\dot{\sigma} + \sigma^{1/2}/C)] \sigma^{-1/2} = A\Theta(\sigma)\sigma^{-1/2}, \quad (1)$$

where A is called the fold coefficient. To estimate¹⁶ A , consider the time evolution of CDM particles which are falling out of a galactic halo for the n th time and then falling back in. Let R_n be the n th turn-around radius. We assume that the rotation curve of the galaxy is flat near $r = R_n$ with time-independent rotation velocity v_{rot} . Then, using the force per unit mass $\vec{f}(r) = -v_{\text{rot}}^2 \hat{r}/r$ and conservation of energy per unit mass $E = \frac{1}{2}\dot{\vec{r}}^2 + V(r)$, the gravitational potential $V(r)$ is calculated as $V(r) = v_{\text{rot}}^2 \ln(r/R_n) + E$. Thus, the particles have a trajectory $\vec{r}(t)$ such that $|\dot{\vec{r}}| = v_{\text{rot}} \sqrt{2 \ln(R_n/r)}$. Here, we neglected the angular momentum of the particles, since at the turaround the particles are far from their distance of closest approach to the galactic center. Finally, we assume that the flow is stationary. This means the number of particles flowing per unit solid angle and per unit time, $dN/d\Omega dt$, is independent of t and r , and hence, the caustic is located exactly at the $(n + 1)$ th turnaround radius R_n . The mass density of particles, $d_n(r)$, follows from the equality: $2dM = d_n(r)r^2 d\Omega \dot{r} dt$. The factor of two appears because there are two distinct flows, out and in. Near the n th outer caustic where $r = R_n - \sigma$, $\ln(R_n/r) \simeq \sigma/R_n$. Therefore, $d_n(r) \simeq A_n \Theta(\sigma)\sigma^{-1/2}$ with $A_n = \sqrt{2}(dM/d\Omega dt|_n) v_{\text{rot}}^{-1} R_n^{-3/2}$. In a self-similar infall, R_n and A_n are estimated¹⁶ as

$$\{R_n : n = 1, 2, \dots\} \simeq (240, 120, 90, 70, 60, \dots) \text{ kpc} \cdot \left(\frac{v_{\text{rot}}}{220 \text{ km/s}}\right) \left(\frac{0.7}{h}\right), \quad (2)$$

$$\{A_n : n = 1, 2, \dots\} \sim (2, 2, 2, 3, 3, \dots) \cdot \frac{10^{-5} \text{ gr}}{\text{cm}^2 \text{ kpc}^{1/2}} \cdot \left(\frac{v_{\text{rot}}}{220 \text{ km/s}}\right)^{1/2} \left(\frac{h}{0.7}\right)^{3/2}. \quad (3)$$

Evidence for the first outer CDM caustic was recently found¹² in the NGC 5846 group of galaxies. The plot of the surface number density of galaxies was inferred to

8 *V. K. Onemli*

mark the first outer caustic of radius R_1 by an abrupt density drop and a transition from a large δv to a very small δv , as predicted by the CDM infall models.²²

3.2. Caustic rings

Caustic rings were first noted as topological circles in Ref. 8, but their properties were left unexplored there. In Ref. 10 they were studied more precisely as closed tubes whose transverse cross-section is a D_{-4} catastrophe; see Fig. 1. Treatment of caustic rings, from the catastrophe theory point of view, is given in Ref. 19. Caustic rings are made up of three fold caustics joining at three topological circle of dual cusp (A_{-3}) catastrophes. Inside (outside) the caustic rings, there are four (two) flows. For simplicity, we consider caustic rings which are axially symmetric about the z direction as well as reflection symmetric with respect to $z = 0$ plane. The CDM flow in that case is effectively two dimensional. In galactocentric cylindrical coordinates, the flow near such a ring is described by:

$$\begin{aligned}\rho(\chi_1, \chi_2) &= a + \chi_1^2 - \chi_2^2, \\ z(\chi_1, \chi_2) &= 2\zeta(\sqrt{p} - \chi_1)\chi_2,\end{aligned}\quad (4)$$

where $\chi_1 = \sqrt{\frac{u}{2}}(\tau_0 - \tau)$, $\chi_2 = \sqrt{\frac{s}{2}}\alpha$. ρ is distance to the z -axis. The parameters τ and α label the particles in the flow. τ is the time a particle crosses the $z = 0$ plane. α is the declination of the particle, relative to the $z = 0$ plane, when it was at last turnaround. a is the radius of the caustic ring. The constants b, s, u and τ_0 are the other characteristics. $\zeta \equiv \frac{b}{\sqrt{us}}$, and $p \equiv \frac{1}{2}u\tau_0^2$ is the longitudinal dimension of the caustic ring cross-section.^e The number density of particles in physical space

$$d(\rho, z, t) = \frac{1}{2\pi\rho} \sum_{j=1}^{n(\rho, z, t)} \frac{d^2N}{d\chi_1 d\chi_2} (\vec{\chi}_j(\rho, z, t)) \frac{1}{|D_2(\vec{\chi})|} \Big|_{\vec{\chi}=\vec{\chi}_j(\rho, z, t)}, \quad (5)$$

where $\vec{\chi} \equiv (\chi_1, \chi_2)$, and $\vec{\chi}_j \equiv (\chi_1, \chi_2)_j$, with $j = 1 \dots n$, are the solutions of $\rho = \rho(\chi_1, \chi_2; t)$ and $z = z(\chi_1, \chi_2; t)$. The number of distinct solutions (flows) n , is a function of the location in space ρ, z , and time t . For the flow near caustic rings, the determinant of the Jacobian matrix

$$D_2 = -4\zeta \left[(\chi_1 - \sqrt{p}/2)^2 + \chi_2^2 - p/4 \right]. \quad (6)$$

Caustic rings occur where D_2 vanishes, i.e. where the map $(\chi_1, \chi_2) \rightarrow (\rho, z)$ is singular. Hence, at the caustic, the density diverges in the limit of zero velocity dispersion. In the parameter space of χ_1 and χ_2 , the curve for which $D_2 = 0$ is a circle centered at $(\chi_1, \chi_2) = (\sqrt{p}/2, 0)$ with radius $\sqrt{p}/2$. A one-parameter representation of this critical circle can be given¹⁹ as:

$$\chi_1 = \frac{\sqrt{p}}{2} (1 + \cos \psi), \quad \chi_2 = \frac{\sqrt{p}}{2} \sin \psi, \quad (7)$$

^eIf $\zeta = 1$, the caustic ring cross-section is a triaxial tricusp.

where the angular variable $\psi \in [0, 2\pi]$. Substituting Eq. (7) into Eqs. (4) yields the equations that describe the cross-section of the caustic ring in the (ρ, z) -plane

$$\rho(\psi) = a + \frac{p}{2} \cos \psi (1 + \cos \psi), \quad z(\psi) = \zeta \frac{p}{2} \sin \psi (1 - \cos \psi). \quad (8)$$

Figure 1 shows a plot of this cross-section. The cusps occur at $\psi = 0, 2\pi/3, 4\pi/3$. In a self-similar infall, the caustic ring radii are estimated⁹ as

$$\{a_n : n = 1, 2, \dots\} \simeq (39, 19.5, 13, 10, 8, \dots) \text{kpc} \cdot \left(\frac{j_{\max}}{0.27}\right) \left(\frac{0.7}{h}\right) \left(\frac{v_{\text{rot}}}{220 \text{ km/s}}\right), \quad (9)$$

where j_{\max} is a parameter proportional to the amount of angular momentum that the particles have, h is the present Hubble constant in units of 100 km/(s Mpc) and v_{rot} is the rotation velocity of the galaxy. Because the caustic rings lie close to the galactic plane, they cause bumps in the rotation curve, at the locations of the rings. In a study of 32 extended and well-measured external galactic rotation curves, evidence was found for the law given in Eq. (9).¹³ In the rotation curve of the Milky Way, the locations of eight sharp rises fit the prediction of the self-similar model at the 3% level.¹⁴ Moreover, a triangular feature in the Infrared Astronomy Satellite (IRAS) map of the Milky Way plane was interpreted as the imprint on baryonic matter of the fifth caustic ring.¹⁴ This nearby ring is 55 pc away from us. The feature is correctly oriented with respect to the galactic plane and the galactic center. Its location is consistent with the bump between 8.28 kpc and 8.43 kpc in the rotation curve. The probability that the coincidence in position of the feature with a rise in the rotation curve is less than 10^{-3} .

The density profile near the caustic ring along the direction $\hat{\sigma}$ perpendicular to the surface is $d(\psi, \sigma) = A(\psi)\Theta(\sigma)\sigma^{-1/2}$, where the fold coefficient

$$A(\psi) = \frac{d^2 M}{d\Omega dt} \sqrt{\frac{2\zeta}{p}} \frac{\cos \alpha(\psi)}{bC(\psi)\rho(\psi)}, \quad (10)$$

with¹⁹

$$C(\psi) = \sqrt{\left| (1 + 2 \cos \psi) \tan \frac{\psi}{2} \right| \sqrt{(1 + \cos \psi)^2 + \zeta^2 \sin^2 \psi}}. \quad (11)$$

The fold coefficients are estimated as a function of location on the ring as

$$\begin{aligned} \{A_n(\psi) : n = 1, 2, \dots\} &\sim (5, 6, 6, 7, 8, \dots) \cdot 10^{-4} \cdot \frac{\mathcal{F}_n(\psi) \text{ gr}}{\text{cm}^2 \text{ kpc}^{\frac{1}{2}}} \\ &\times \left(\frac{0.27}{j_{\max}}\right)^{\frac{3}{2}} \left(\frac{h}{0.7}\right)^{\frac{3}{2}} \left(\frac{v_{\text{rot}}}{220 \text{ km/s}}\right)^{\frac{1}{2}}, \end{aligned} \quad (12)$$

where¹⁹

$$\mathcal{F}_n(\psi) = \frac{[1 + \frac{p_n}{2a_n} \cos \psi (1 + \cos \psi)]^{-1}}{\sqrt{\left| (1 + 2 \cos \psi) \tan \frac{\psi}{2} \right| [(1 + \cos \psi)^2 + \zeta_n^2 \sin^2 \psi]^{\frac{1}{2}}}}. \quad (13)$$

Due to the symmetry of the tricusp with respect to the $z = 0$ axis, we have $\mathcal{F}_n(\vartheta) = \mathcal{F}_n(-\vartheta)$ and $\mathcal{F}_n(\frac{2\pi}{3} \pm \vartheta) = \mathcal{F}_n(\frac{4\pi}{3} \mp \vartheta)$. For the typical values $p_n = 0.1$, a_n and $\zeta_n = 1$, near the outer cusp $\mathcal{F}(\vartheta) \simeq 0.525 \vartheta^{-\frac{1}{2}}$. Near the nonplanar cusps $\mathcal{F}(\frac{2\pi}{3} \pm \vartheta) \simeq 0.585 \vartheta^{-\frac{1}{2}}$. This $\vartheta^{-\frac{1}{2}}$ divergence of the fold coefficients at the cusps is cut off when $\delta v \neq 0$, because, the location of the caustic surface gets smeared over some distance δx and the cusps are smoothed out. For CDM caustics in galactic halos, δx and δv are related^{9,15,16} as $\delta x \sim R \delta v/v$ where v is the order of magnitude of the velocity of the particles in the flow and R is the distance scale over which that flow turns around. For a galaxy like our own, $v = 500$ km/s and $R = 200$ kpc are typical orders of magnitude. As a result of primordial velocity dispersion, axion and WIMP caustics in galactic halos are typically smeared over $\delta x_a \sim 6 \cdot 10^4$ km $(10^{-5} \text{eV}/m_a)^{5/6}$ and $\delta x_\chi \sim 10^{10}$ km $(\text{GeV}/m_\chi)^{1/2}$, respectively. However, a CDM flow may have an effective velocity dispersion δx_{eff} which is larger than its primordial velocity dispersion. Effective velocity dispersion occurs when the sheet on which the dark matter particles lie in phase space is wrapped up on sub-scales that are small compared to the galaxy as a whole. Little is known about the size of the δx_{eff} in galactic halos. However, the widths of the bumps at the ring locations in the rotation curve of the Milky Way and the sharpness of the edges of the triangular feature in the IRAS map were used to deduce an upper bound of 15-20 pc on δx_{eff} at most.¹⁴

I use the primordial smearing distances δx_a and δx_χ to estimate the upper limits for the fold coefficient and for the lensing effects at the cusps of caustic rings as follows. I set the δv of the particle species equal to zero, and then calculate the fold coefficients and the lensing effects (Sect. 4) on the caustic surface at a point whose transverse distances $\Delta\rho$ and Δz to the nearby cusp—that would occur in the limit $\delta v = 0$ —are slightly greater than the primordial smearing out distance δx_a or δx_χ . These points correspond to the locations that are respectively $\Delta\psi = \frac{\pi}{7500}$ and $\Delta\psi = \frac{\pi}{75}$ radian away from the cusps in the axionic and WIMPic cases, respectively. Similarly, I use the upper bound for the smearing distance δx_{eff} to estimate the lower limits: I choose a point which is about the maximum smearing distance δx_{eff} away from the nearby cusp and calculate the fold coefficients and the lensing effects there. Such points differ by $\Delta\psi = \frac{\pi}{7.5}$ radians from the cusp locations. The calculations¹⁹ show that, for the axion caustic rings, the factor $\mathcal{F}(\psi)$ may change the estimates given for the A_n in Eq. (12) between 0.8 and 26 times at the outer cusp, and between 0.9 and 29 times at the nonplanar cusps. The upper bounds of A_n for the WIMP caustic rings, on the other hand, are ten times less than the upper bounds for the axionic rings.

4. Gravitational Lensing by the CDM Caustics

Matter curves the spacetime. As a result, light rays coming from a background source are deflected due to the presence of a forefront object. This effect is known as gravitational lensing. Choosing the y -axis in the direction of propagation of light,

the angular shift in the position of the source $\vec{\xi}_S \equiv (\xi_{Sx}, \xi_{Sz})$ due to a lens is given by $\Delta\xi \equiv \vec{\xi}_I - \vec{\xi}_S = \vec{\nabla}_{\xi_I} \Phi(\vec{\xi}_I)$, where $\vec{\xi}_I \equiv (\xi_{Ix}, \xi_{Iz})$ is the position of the image with lens present. The 2D potential Φ is solved from the Poisson equation $\nabla_{\xi_I}^2 \Phi = 2\Sigma/\Sigma_c$, where column density Σ and the critical surface density Σ_c are defined as:

$$\Sigma(\vec{\xi}_I) = \int dy d(D_L \xi_{Ix}, y, D_L \xi_{Iz}),$$

$$\Sigma_c = \frac{c^2 D_S}{4\pi G D_L D_{LS}} = 0.347 \frac{\text{g}}{\text{cm}^2} \left(\frac{D_S}{D_L D_{LS}} \text{Gpc} \right). \quad (14)$$

Here, D_L and D_S are the distances of the observer to the lens and to the source, respectively. D_{LS} is the distance of the source to the lens. The image distortion and magnification are given by the Jacobian matrix of the map $\vec{\xi}_S(\vec{\xi}_I)$. Because gravitational lensing does not change surface brightness, the magnification \mathcal{M} is the ratio of image area to source area. Hence, $\mathcal{M} = 1/|\det(\partial\xi_{Si}/\partial\xi_{Ij})|$, which yields, to first order, $\mathcal{M} = 1 + 2\Sigma/\Sigma_c$. Gravitational lensing has proven useful in revealing the massive compact halo objects (MACHOs) in galaxies and constraining the mass distribution in galaxy clusters. For some recent interesting lensing applications see Refs. 23. Dark matter caustics have calculable lensing signatures.^{15–19} The caustic ring model^{8–10} precisely predicts the density and the geometry of the CDM distribution in caustic neighborhood. In Ref. 16, we derived the lensing equations for the line of sights that are parallel to the galactic plane of a caustic ring and near tangent to its surface in some specific cases. In Ref. 19, I obtained the lensing equations for the same line of sights, but near tangent to a caustic ring *anywhere* on the surface and estimated the lensing effects near the cusps of axion and WIMP caustic rings. Here, I summarize these effects.

The gravitational lensing effects of a caustic are largest when the line of sight is near tangent to the surface, because the contrast in column density Σ is largest there. For such line of sights, the associated fold of outer caustics, in general, and of caustic rings, in the regions where $0 < \psi < 2\pi/3$ and $4\pi/3 < \psi < 2\pi$, are curved towards the side with the two extra flows; see Fig. 4.^f In these cases, the image shift and magnification are given¹⁶ as

$$\Delta\xi = \xi_I - \xi_S = \eta \xi_I \Theta(-\xi_I), \quad \mathcal{M} = \frac{d\xi_I}{d\xi_S} = 1 + \eta \Theta(-\xi_I) + O(\eta^2), \quad (15)$$

where

$$\eta = \frac{2\pi A \sqrt{2|R|}}{\Sigma_c}. \quad (16)$$

Here R is the curvature radius of the surface along the direction associated with the chosen line of sight. Hence, when the line of sight of a moving source crosses

^fIf the line of sight is near tangent to the ring surface at $\psi \in [\frac{2\pi}{3}, \frac{4\pi}{3}]$, the associated fold is curved away from the side with the two extra flows. The expected effects are not as large in that case.^{16,19}

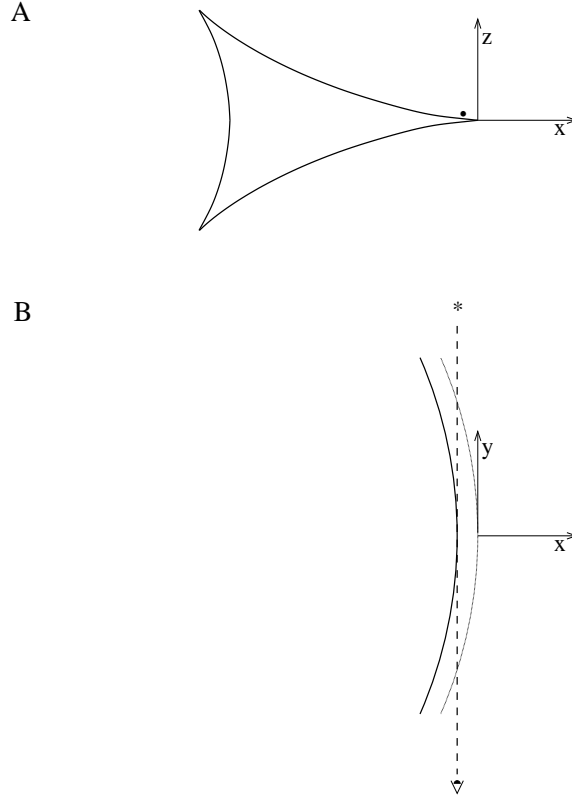
12 *V. K. Onemli*


Fig. 4. Lensing by a caustic ring for a line of sight near tangent to the surface at a given point ψ_* close to the outer cusp. The line of sight lies in the $z = z(\psi_*)$ -plane. A) Side view in the direction of the line of sight. The latter is represented by the dot near $x = z = 0$. B) Top view.

the caustic, the component of its apparent velocity perpendicular to the surface and the magnification of the image changes abruptly. Both affects are of order η .

The η_n for the outer caustics are estimated,¹⁶ using Eqs. (2) and (3) in Eq. (16), as

$$\{\eta_n : n = 1, 2, \dots\} \sim (7, 6, 6, 5, 5, \dots) \cdot 10^{-3} \times \left(\frac{D_L D_{LS}}{D_S \text{ Gpc}} \right) \left(\frac{v_{\text{rot}}}{220 \text{ km/s}} \right) \left(\frac{h}{0.7} \right) . \quad (17)$$

Lensing effects are always maximum when the lens is situated half-way between the source and the observer. Also, D_S should be as large as possible to get the largest effects. Therefore, in my estimates, I will assume that the source is at cosmological distances, e.g. $2D_L = 2D_{LS} = D_S = 1$ Gpc. For the outer caustics, this yields a magnification of order 10^{-3} which can not be detected by present instruments. However, the images of extended sources may be modified in recognizable ways.^{15,16} In particular, if a straight jet makes angle α with the normal, it appears bent by an angle $\eta \sin(2\alpha)/2$ where its line of sight crosses a fold of an outer caustic.¹⁶

For the caustic rings, A is given in Eq. (10). Along the chosen line of sights, the curvature radius of the associated fold¹⁹

$$R = -\zeta^{-1} \text{Sign}(\cos \psi - \cos 2\psi) \left[a + \frac{p}{2} \cos \psi (1 + \cos \psi) \right] (\zeta^2 + \cot^2 \frac{\psi}{2})^{\frac{1}{2}}. \quad (18)$$

Therefore¹⁹

$$\eta = \frac{4\pi}{\Sigma_c} \frac{d^2 M}{d\Omega d\tau} \frac{\cos \alpha(\psi)}{b\sqrt{ap}} \mathcal{G}(\psi), \quad (19)$$

where

$$\mathcal{G}(\psi) = \sqrt{\frac{|\csc \psi|}{\left[1 + \frac{p}{2a} \cos \psi (1 + \cos \psi)\right] |(1 + 2 \cos \psi) \tan \frac{\psi}{2}|}}. \quad (20)$$

The $\eta_n(\psi)$ for the rings are estimated¹⁹ as

$$\begin{aligned} \{\eta_n(\psi) : n = 1, 2, \dots\} &\sim (7, 6, 6, 5, 5, \dots) \cdot 10^{-2} \mathcal{G}_n(\psi) \frac{D_L D_{LS}}{D_S \text{ Gpc}} \\ &\times \left(\frac{0.27}{j_{\max}} \right) \left(\frac{h}{0.7} \right) \left(\frac{v_{\text{rot}}}{220 \text{ km/s}} \right). \end{aligned} \quad (21)$$

In the limit of zero velocity dispersion $\mathcal{G}(\psi)$ diverges at the cusps. $\mathcal{G}(\vartheta) \simeq 0.8 \vartheta^{-1}$, whereas $\mathcal{G}(2\pi/3 - \vartheta) \simeq 0.6 \vartheta^{-1/2}$. Hence, the effects are large near the cusps, in particular near the outer cusp. For the line of sights near tangent to a cosmological ring surface in the region $-\pi/27 < \psi < \pi/27$, the magnification is more than 10%. Effects of that order can be observed by present instruments.²⁴

The lensing effects of the cusps of axion and WIMP caustic rings may be estimated¹⁹ by turning the δv of the particle species on, as described in Sect. 3.2. At the outer cusp of a cosmological axion caustic ring, the range of η is constrained between $\eta(\pm \frac{\pi}{7.5}) \simeq 2.9 \cdot 10^{-2}$ and $\eta(\pm \frac{\pi}{7500}) \simeq 27.9$. This implies a magnification between 3% and 2800%. At the outer cusp of a cosmological WIMP caustic ring, on the other hand, the range is constrained between $\eta(\pm \frac{\pi}{7.5}) \simeq 0.029$ and $\eta(\pm \frac{\pi}{75}) \simeq 0.28$. This implies a magnification between 3% and 28% at the outer cusp. The lower bound of η at the nonplanar cusps of cosmological caustic rings is $\eta(\frac{2\pi}{3} - \frac{\pi}{7.5}) \simeq 0.016$. For a cosmological axion caustic ring, the upper bound is $\eta(\frac{2\pi}{3} - \frac{\pi}{7500}) \simeq 0.46$. Thus, the magnification can be between 2% and 46% at the nonplanar cusps. (Twenty five MACHOs were discovered²⁴ by magnifications that range between 12% and 46%). For a cosmological WIMP caustic ring, on the other hand, $\eta(\frac{2\pi}{3} - \frac{\pi}{75}) \simeq 0.046$, hence the magnification can be between 2% and 5% at the nonplanar cusps.

Pointlike background sources may probe the CDM caustics, as they cross behind the cusps of a foreground halo. The time scale δt for the brightness to change is about the transit time of a background source across the thickness (i.e. smearing out distance) δx of the caustic edges. For axion caustics δt_a is about an hour, whereas for WIMP caustics δt_χ is about a year.¹⁵ A strategy to detect the caustics may be a MACHO style experiment: monitoring large number of pointlike background

sources behind the disks of foreground halos and watching for their edge crossings near the cusps. The number of outer caustics across the face of a halo is about the number of orbits (discrete flows) since it is formed,^{5,15} say $N \approx 10$ to 100. The number of caustic rings are of the same order, because, the very same flows that generate the outer caustics, generate the caustic rings.⁵ Caustic ring radii $a_n \sim 40/n$ kpc. Each background source traverses such a distance scale about $10^8/n$ years. So monitoring 10^8 stars for a year will show about 20 to 200 crossings of the ring edges. Only 6% of the ring surface (near the cusps) can magnify the sources more than 10%, hence about 1 to 10 cusp crossings may be detected in a year. Note that I estimated the prospects considering the minimal cusp structure predicted by the caustic ring model. Cusps are generic and common throughout the halos. More background sources may easily pass behind the generic cusps of a foreground halo.

5. Conclusions

Caustics are common features in the propagation of light, because photons are collisionless and flow of light from a point source has zero velocity dispersion. In the occasions where these two conditions are satisfied, caustics in the flow of the ordinary luminous matter are also observed. Cold dark matter (CDM) flow onto isolated galaxies has both of the properties; the particles interact only weakly and the flow has a tiny velocity dispersion. Therefore, caustic formation in the halos of CDM is inevitable. Gravitational lensing effects of the cusps at cosmological distances may be detected by present instruments. Caustic ring model of galactic halos predicts the geometry and density near the cusps of the rings. I derived the lensing equations for the line of sights near tangent to a caustic ring anywhere on the surface, and estimated the lensing effects near its cusps. For a cosmological axion caustic ring, the magnification may range between 3% and 2800% at the outer cusp, and between 2% and 46% at the nonplanar cusps. For a cosmological WIMP caustic ring, on the other hand, the magnification may range between 3% and 28% at the outer cusp, and between 2% and 5% at the nonplanar cusps. As pointlike background sources pass behind the caustics of foreground halos, the time scales for brightness to change is about an hour for the axion folds and about a year for the WIMP folds. Hence, depending on the strength of the observed effect and the time scale for brightness change, it may even be possible to discriminate between the axions and the WIMPs.

Acknowledgments

This research was supported by European Union Commission Marie Curie Fellowship FP-6-012679.

⁵The sharp rises in the rotation curve of the Milky Way imply the existence of 13 caustic rings.¹⁴

References

1. A thorough review can be found in J. F. Nye, *Natural Focusing and Fine Structure of Light* (Institute of Physics Publishing, Bristol, 1999).
2. D. F. Malin and D. Carter, *Nature* **285**, 643 (1980).
3. L. Hernquist and P. J. Quinn, *Astrophys. J.* **312**, 1 (1985); E. Bertschinger, *Astrophys. J. Suppl.* **58**, 39 (1985); J. Binney and S. Tremaine, *Galactic Dynamics* (Princeton University Press, 1987); A. Natarajan and P. Sikivie, *Phys. Rev.* **D72**, 083513 (2005).
4. D. N. Spergel et al., astro-ph/0603449.
5. P. Sikivie and J. R. Ipser, *Phys. Lett.* **B291**, 288 (1992).
6. P. Sikivie, I. Tkachev and Y. Wang, *Phys. Rev. Lett.* **75**, 2911 (1995).
7. Y. B. Zel'dovich, *Astrofizika* **6**, 319 (1970); *Astron. Astrophys.* **5**, 84 (1970).
8. P. Sikivie, I. Tkachev and Y. Wang, *Phys. Rev.* **D56**, 1863 (1997)
9. P. Sikivie, *Phys. Lett.* **B432**, 139 (1998).
10. P. Sikivie, *Phys. Rev.* **D60**, 063501 (1999).
11. S. Tremaine, *Mon. Not. R. Astron. Soc.* **307**, 877 (1999).
12. A. Mahdavi, N. Trentham and R. B. Tully, astro-ph/0506737; R. B. Tully, astro-ph/0509482.
13. W. Kinney and P. Sikivie, *Phys. Rev.* **D61**, 087305 (2000).
14. P. Sikivie, *Phys. Lett.* **B567**, 1 (2003).
15. C. Hogan, *Astrophys. J.* **527**, 42 (1999).
16. C. Charmousis, V. Onemli, Z. Qiu and P. Sikivie, *Phys. Rev.* **D67**, 103502 (2003).
17. Vakif K. Onemli, astro-ph/0401162, Ph. D. thesis, to be published by the Nova Science Publishers, Inc., New York.
18. R. Gavazzi, R. Mohayaee and B. Fort, *Astron. Astrophys.* **445**, 43 (2006); R. Mohayaee, S. Colombi, B. Fort, R. Gavazzi, S. Shandarin and J. Touma, astro-ph/0510575.
19. V. K. Onemli, *Phys. Rev.* **D74**, 123010 (2006), astro-ph/0510414.
20. P. Sikivie and S. Wick, *Phys. Rev.* **D66**, 023504 (2002).
21. S. Chang, C. Hagmann and P. Sikivie, *Phys. Rev.* **D59**, 023505 (1999).
22. J. A. Fillmore and P. Goldreich, *Astrophys. J.* **281**, 1 (1984); E. Bertschinger, *Astrophys. J. Suppl.* **58**, 39 (1985).
23. K. K. Nandi, Y.-Z. Zhang and A. V. Zakharov, *Phys. Rev.* **D74**, 024020 (2006); M. Fairbairn, astro-ph/0511085.
24. C. Thomas et al., *Astrophys. J.* **631**, 906 (2005).